

CHEMISTRY OF MATERIALS

VOLUME 20, NUMBER 8

APRIL 22, 2008

© Copyright 2008 by the American Chemical Society

Communications

Nano-Pt Modified Aligned Carbon Nanotube Arrays Are Efficient, Robust, High Surface Area Electrocatalysts

Yong Liu,[†] Jun Chen,^{*,†} Weimin Zhang,[†] Zifeng Ma,[‡]
Gerhard F. Swiegers,^{*,§} Chee O. Too,[†] and
Gordon G. Wallace^{*,†}

ARC Centre of Excellence for Electromaterials Science,
Intelligent Polymer Research Institute, University of
Wollongong, New South Wales 2522, Australia, Institute of
Electrochemical Engineering and Technology, Shanghai Jiao
Tong University, Shanghai 200240, China, and CSIRO
Molecular and Health Technologies, Bag 10, Clayton,
Victoria 3169, Australia

Received December 6, 2007

Revised Manuscript Received January 24, 2008

Heterogeneous, precious metal catalysts in electrochemical devices like methanol or H₂/O₂ fuel cells are typically relatively inefficient per metal atom present. In most metallic Pt catalysts, for example, the majority of atoms lie within the bulk of the metal and are therefore unable to participate in the catalysis. A large scale uptake of current fuel cell technology would, consequently, require an annual production of Pt greater than the total mined to date.¹ Pt replacement technologies or catalytic structures with greater atom efficiency are needed.¹ A possible solution to this problem is to thinly coat precious metal catalysts onto electrically conducting supports having high surface areas. Carbon nanotubes offer important opportunities in this respect. For example, metal nanoparticles supported on carbon nanotubes

exhibit substantial enhancements in catalytic activities,² maximum power densities,^{3,4} and excellent selectivity in commercially important processes, such as the electrooxidation of methanol.⁵ Of particular interest are *perpendicularly aligned carbon nanotubes* (ACNTs).⁶ ACNTs have special advantages over their randomly aligned counterparts. These include larger and better-defined surface areas, as well as a capacity for controlled surface modification using various transduction materials.^{7,8} But how could an array of aligned, multiwall carbon nanotubes be turned into an electrocatalyst? Moreover, would such an array survive the often dramatic physical stresses created by mass transport during catalysis?⁹ In this work we describe a free-standing, conductive ACNT array that, when coated with Pt nanoparticles, acts as an efficient and astonishingly robust electrocatalyst.

In previous work we described a technique for depositing an extended array of perpendicularly aligned carbon nanotubes on a flexible PVDF membrane.¹⁰ The process involved growing a “forest” of aligned, multiwall carbon nanotubes on a quartz plate by pyrolysis of iron(II) phthalocyanine using thermal chemical vapor deposition (Scheme 1a).⁶ A coating of poly(vinylidene fluoride) (PVDF) was then cast on the

(2) For example, Wu, G.; Xu, B.-Q. *J. Power Sources* **2007**, *174*, 148. (see especially Figure 10a). See also Freemantle, M. *Chem. Eng. News* **1996**, *74*, 62.

(3) For example, Li, W.; Liang, C.; Qiu, J.; Zhou, W.; Han, H.; Wei, Z.; Sun, G.; Xin, Q. *Carbon* **2002**, *40*, 787.

(4) For example, Li, W.; Liang, C.; Zhou, W.; Qiu, J.; Zhou, Z.; Sun, G.; Xin, Q. *J. Phys. Chem. B* **2003**, *107*, 6292.

(5) For example, Liao, S.; Holmes, K. A.; Tsapralis, H.; Birss, V. H. *J. Am. Chem. Soc.* **2006**, *128*, 3504.

(6) Huang, S.; Dai, L.; Mau, A. W. H. *J. Phys. Chem. B* **1999**, *103*, 4223.

(7) Dai, L.; Patil, A.; Gong, X.; Guo, Z.; Liu, L.; Liu, Y.; Zhu, D. *ChemPhysChem* **2003**, *4*, 1150.

(8) He, P.; Dai, L. *Chem. Commun.* **2004**, 348.

(9) For example, Ertl, G. *Science* **1991**, *254*, 1751.

(10) Chen, J.; Minett, A. I.; Lynam, C.; Wang, J.; Wallace, G. G. *Chem. Mater.* **2007**, *19*, 3595.

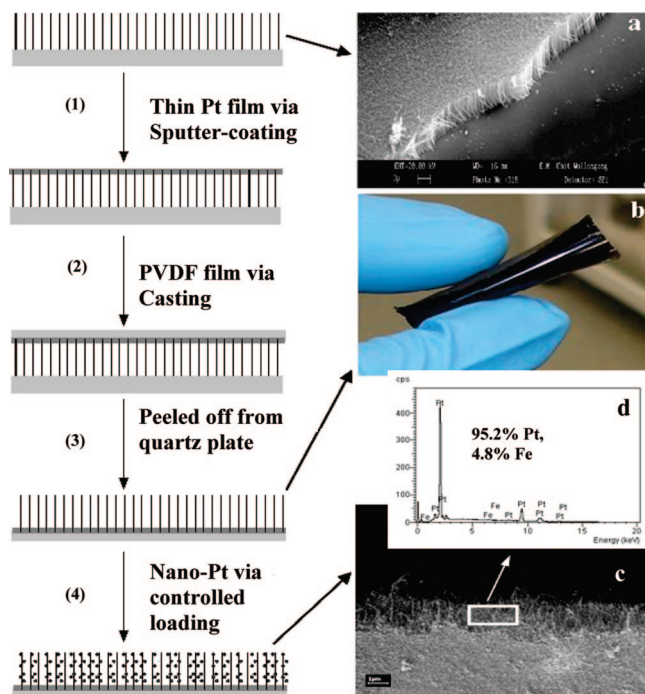
[†] University of Wollongong.

[‡] Shanghai Jiao Tong University.

[§] CSIRO Molecular and Health Technologies.

(1) McNicol, B.; Rand, D.; Williams, K. *J. Power Sources* **1999**, *83*, 15.

Scheme 1



top of the nanotubes. When this layer was subsequently peeled off the quartz, it retained the ACNTs, yielding a flexible PVDF membrane with an ACNT array surface.¹⁰ The resulting membrane was, however, poorly conductive (1–10 k Ω/\square); this severely limited its electrochemical utility. To overcome this constraint, we varied the technique to include, after the CVD process, a step in which a thin layer of Pt was sputter-coated onto the upper surface of the ACNT array (step (1) in Scheme 1). This coating, which was <100 nm thick, provided an electrical connection between the nanotubes. A PVDF layer was then cast onto the sputter-coated Pt layer (step (2) in Scheme 1). Peeling off the PVDF layer produced a highly conductive, flexible, free-standing ACNT array electrode with low resistance <30 Ω/\square (Scheme 1b). The composite ACNT/Pt/PVDF electrode was remarkably robust; it could be rolled up without excessive damage (Scheme 1b). We were, consequently, interested to see if this electrode could be used as an electrocatalyst or if the physical delicacy of the ACNT array was such that it would rapidly degrade during catalysis.

To this end, Pt nanoparticles were electrodeposited on the ACNT array by cyclic voltammetry from 0.01 M H₂PtCl₆/0.5 M NaNO₃/H₂O, undertaken between 0.0 and +0.6 V (vs Ag/AgCl) at a scan rate of 0.05 V s⁻¹. The SEM image in Scheme 1c shows that Pt nanoparticles were deposited along the outside wall of the individual nanotubes. No Pt film was formed on the top of ACNT array. EDX analysis (Scheme 1d) indicated that the ACNT array contained 95.2% Pt and 4.8% Fe (from the catalysts used for CNT growth), confirming the electrodeposition of Pt.

The resulting nano-Pt-ACNT/Pt/PVDF electrode was characterized in a standard three-electrode cell with a Ag/AgCl reference electrode and a RVC auxiliary electrode. Solutions were deoxygenated with N₂ for 15 min prior to the experiments and then maintained under inert atmosphere.

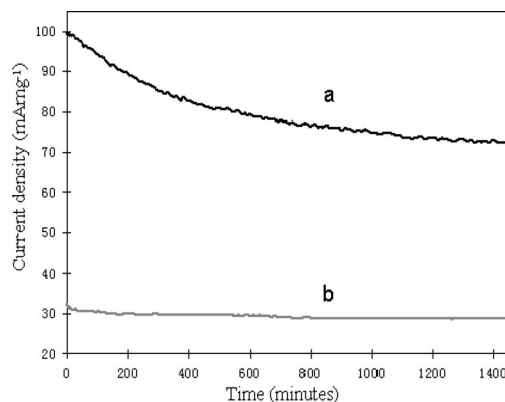


Figure 1. Chronoamperogram of methanol oxidation at (a) nano-Pt loaded ACNT/Pt/PVDF and (b) ACNT/Pt/PVDF at a potential of +0.67 V.

The electrochemically active specific surface area (EASSA) of the Pt in the resulting electrode was determined by calculating the charge transfer involved in H₂ adsorption and desorption during cycling (Figure S1, Supporting Information).¹¹ Before electrodeposition of the Pt nanoparticles, the ACNT/Pt/PVDF electrode exhibited an EASSA of 9 m² g⁻¹ Pt (due to the sputter-coated Pt layer). This is lower than Pt black (20–26 m² g⁻¹) and platinized Pt films (2–30 m² g⁻¹).¹² Following electrodeposition, the EASSA of the electrodeposited Pt nanoparticles on the PVDF/ACNT array was found to be 143 ± 14.3 m² g⁻¹. This is more than the typical nanostructured Pt film (38 m² g⁻¹),¹³ mesoporous Pt powders (60 m² g⁻¹),¹⁴ and Pt/C (14–87 m² g⁻¹).¹⁴ It is also more than typical electrodes comprising nonaligned, multiwalled carbon nanotubes (e.g., 101 m² g⁻¹ in ref 2). To place these quantities in context, carbon-based support materials having EASSAs of up to 800 m² g⁻¹ C are known.¹⁵

Cyclic voltammetry in 1 M CH₃OH/1 M H₂SO₄/H₂O solution indicated that the nano-Pt-ACNT/Pt/PVDF electrode displayed dramatically enhanced performance and a more negative starting potential for methanol oxidation than an ITO electrode that had been sputter-coated with Pt (Figure S2, Supporting Information).

Potentiostatic investigations (+0.67 V) further compared the current due to methanol oxidation catalysis (producing CO₂) at the ACNT/Pt/PVDF electrode with and without nano-Pt modification. As shown in Figure 1a, after an initial decline, the current density at the nano-Pt-ACNT/Pt/PVDF leveled off, yielding a current density after 24 h of 73 mA cm⁻² of total Pt present. By contrast, the unmodified ACNT/Pt/PVDF electrode displayed a current density of 29

- (11) Larminie, J.; Dicks, A. *Fuel Cell Systems Explained*; Wiley: New York, 2000.
- (12) Feltham, A. M.; Spiro, M. *Chem. Rev.* **1971**, *71*, 187. Bett, J.; Lundquist, J.; Washington, E.; Stonehart, P. *Electrochim. Acta* **1973**, *18*, 343.
- (13) Gollas, B.; Elliott, J. M.; Bartlett, P. N. *Electrochim. Acta* **2000**, *43*, 3711.
- (14) Attard, G. S.; Göltner, C. G.; Corker, J. M.; Henke, S.; Templer, R. H. *Angew. Chem., Int. Ed. Engl.* **1997**, *36*, 1315. Attard, G. S.; Coleman, N. R. B.; Elliott, J. M.; Boneviot, L.; Béland, F.; Danumash, C.; Giasson, S.; Kaliaguine, S. *Stud. Surf. Sci. Catal.* **1998**, *117*, 89. Pozio, A.; De Francesco, M.; Cemmi, A.; Cardellini, F.; Giorgi, L. *J. Power Sources* **2002**, *105*, 13.
- (15) For example Wang, J. N.; Zhao, Y. Z.; Niu, J. J. *J. Mater. Chem.* **2007**, *17*, 1151.

$\text{mA} \cdot \text{mg}^{-1}$ after 24 h (Figure 1b). Thus, the Pt nanoparticles on the ACNT array initially contributed $181 \text{ mA} \cdot \text{mg}^{-1}$ for catalytic methanol oxidation; after 24 h this had fallen by 35% to $117 \text{ mA} \cdot \text{mg}^{-1}$. This is 4-fold larger than the equivalent thin-film Pt catalysts deposited via sputter-coating comparable to, or larger than, the mass activity of electrodes fabricated from nonaligned, multiwalled carbon nanotubes. Systems such as that in ref 2 generate a maximum initial current of $170 \text{ mA} \cdot \text{mg}^{-1}$ during cyclic voltammetry; however, potentiostatic data over 24 h have generally not been provided in such studies. The sustained high current of the nano-Pt-ACNT/Pt/PVDF electrode indicates that poisoning by intermediates, such as CO and formaldehydic polymers, is not a significant problem.

The relative efficiency of this catalysis is illustrated by the fact that a standard commercial catalyst for methanol oxidation (E-Tek 20% Ru–Pt (1:1 atomic ratio) on Vulcan XC72R) is reported to achieve an initial current density of $307 \text{ mA} \cdot \text{mg}^{-1}$ at the more positive potential of 0.75 V (1 M CH_3OH /1 M $\text{H}_2\text{SO}_4/\text{H}_2\text{O}$).¹⁶ Poisoning effects typically cause methanol oxidation currents to fall substantially from the initial (sometimes by several orders of magnitude).^{1,17} Thus, the ACNT-supported Pt nanoparticles achieved efficiencies that were similar to those of commercial catalysts without exhaustive optimization. Moreover, they were highly resistant to deactivation over 24 h. This is despite their inopportune pure-Pt composition relative to the Ru–Pt alloys that are best suited to methanol oxidation catalysis.^{1,17}

The atom efficiency and robustness of the nano-Pt-ACNT/Pt/PVDF arrays were confirmed in potentiostatic studies of hydrogen reduction catalysis ($2\text{H}^+ \rightarrow \text{H}_2$). For comparative purposes, this work was carried out in 1 M $\text{H}_2\text{SO}_4/\text{H}_2\text{O}$ at -0.44 V as previously described.¹⁸ At this potential, bubbles of H_2 gas are rapidly and vigorously generated on Pt catalysts. Smooth-surface Pt electrocatalysts typically display

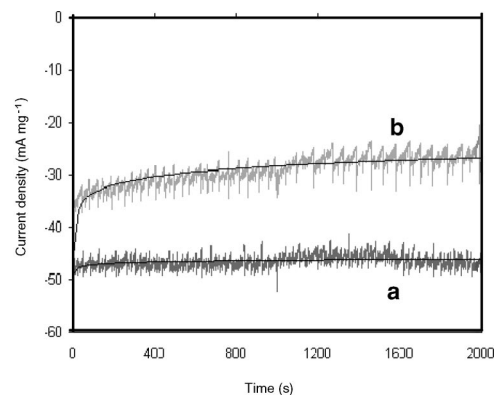


Figure 2. Chronoamperogram of hydrogen generation at (a) nano-Pt loaded ACNT/Pt/PVDF and (b) ACNT/Pt/PVDF at -0.44 V .

declines of approximately 1 magnitude in the rate of H_2 generation during the first 30 min.¹⁸

Figure 2a shows, however, that the nano-Pt-ACNT/Pt/PVDF electrode generated an *invariant* current density of $47 \text{ mA} \cdot \text{mg}^{-1}$ as a result of H_2 generation over the first 30 min. The unmodified ACNT/Pt/PVDF electrode displayed an approximately 40% decline in activity to $26 \text{ mA} \cdot \text{mg}^{-1}$ after 30 min (Figure 2b). Thus, the ACNT-supported nano-Pt is more active per unit EASSA than the sputter-coated Pt. Moreover, the CNT array was clearly not physically degraded by the vigorous bubble formation. Quite the contrary, the array appears to have *assisted* the catalysis by inhibiting deactivation of the Pt.¹⁸ The systematic fluctuations in the current in Figure 2a–b suggest that the CNT array may have regulated the formation and release of the gas bubbles.

These results indicate that arrays of aligned, multiwalled carbon nanotubes are substantially stronger and more sturdy than has hitherto been anticipated. Their morphology, moreover, appears to open new opportunities in the realm of catalysis.

Supporting Information Available: Experimental details, cyclic voltammetry, and Raman spectra (PDF). This material is available free of charge via the Internet at <http://pubs.acs.org>.

CM703471X

(16) Ganesan, R.; Lee, J.-S. *Angew. Chem., Int. Ed.* **2005**, *44*, 6557.

(17) Kua, J.; Goddard, W. A. *J. Am. Chem. Soc.* **1999**, *121*, 10928.

(18) Chen, J.; Huang, J.; Swiegers, G. F.; Too, C. O.; Wallace, G. G. *Chem. Commun.* **2004**, 308. Rapid initial deactivation is also seen in other reactions, for example, Tian, N.; Zhou, Z.-Y.; Sun, S.-G.; Ding, Y.; Wang, Z. L. *Science* **2007**, *316*, 732.